Published in final edited form as:
Cancer Res. 2012 May 15; 72(10): 2554–2564. doi:10.1158/0008-5472.CAN-11-3552.

KRas Induces a Src/PEAK1/ErbB2 Kinase Amplification Loop That Drives Metastatic Growth and Therapy Resistance in Pancreatic Cancer

Jonathan A. Kelber[1,3], **Theresa Reno**[1,3], **Sharmeela Kaushal**[3], **Cristina Metildi**[3,4], **Tracy Wright**[1,3], **Konstantin Stoletov**[1,3], **Jessica M. Weems**[1,3], **Frederick D. Park**[1,2,3], **Evangeline Mose**[3], **Yingchun Wang**[5], **Robert M. Hoffman**[4,6], **Andrew M. Lowy**[3,4], **Michael Bouvet**[3,4], and **Richard L. Klemke**[1,3]

[1]Department of Pathology, UCSD, La Jolla, California

[2]Department of Medicine, UCSD, La Jolla, California

[3]Moores Cancer Center, UCSD, La Jolla, California

[4]Department of Surgery, Division of Surgical Oncology, UCSD, La Jolla, California

[5]Institute of Genetics and Developmental Biology, Chinese Academy of Science, Beijing, China

[6]AntiCancer, Inc., San Diego, California

Abstract

Early biomarkers and effective therapeutic strategies are desperately needed to treat pancreatic ductal adenocarcinoma (PDAC), which has a dismal 5-year patient survival rate. Here, we report that the novel tyrosine kinase PEAK1 is upregulated in human malignancies, including human PDACs and pancreatic intraepithelial neoplasia (PanIN). Oncogenic KRas induced a PEAK1-dependent kinase amplification loop between Src, PEAK1, and ErbB2 to drive PDAC tumor growth and metastasis *in vivo*. Surprisingly, blockade of ErbB2 expression increased Src-dependent PEAK1 expression, PEAK1-dependent Src activation, and tumor growth *in vivo*, suggesting a mechanism for the observed resistance of patients with PDACs to therapeutic intervention. Importantly, PEAK1 inactivation sensitized PDAC cells to trastuzumab and gemcitabine therapy. Our findings, therefore, suggest that PEAK1 is a novel biomarker, critical signaling hub, and new therapeutic target in PDACs.

Corresponding Author: Richard L. Klemke, School of Medicine, UCSD 9500 Gilman Drive #0612, La Jolla, CA 92093. Phone: 858-822-5610; Fax: 858-822-4566; rklemke@ucsd.edu.

Note: Supplementary data for this article are available at Cancer Research Online (http://cancerres.aacrjournals.org/).

Disclosure of Potential Conflicts of Interest
No potential conflicts of interests were disclosed.

Authors' Contributions
Conception and design: J.A. Kelber, S. Kaushal, Y. Wang, R.L. Klemke Development of methodology: J.A. Kelber, T. Reno, S. Kaushal, C. Metildi, T. Wright, K. Stoletov, E. Mose, Y. Wang, A.M. Lowy, R.L. Klemke
Acquisition of data (provided animals, acquired and managed patients, provided facilities, etc.): J.A. Kelber, T. Reno, S. Kaushal, C. Metildi, T. Wright, K. Stoletov, J.M. Weems, F.D. Park, E. Mose, Y. Wang, A.M. Lowy, M. Bouvet, R.L. Klemke
Analysis and interpretation of data (e.g., statistical analysis, biostatistics, computational analysis): J.A. Kelber, S. Kaushal, T. Wright, A.M. Lowy, R.L. Klemke
Writing, review, and/or revision of the manuscript: J.A. Kelber, T. Reno, C. Metildi, K. Stoletov, J.M. Weems, R.M. Hoffman, R.L. Klemke
Administrative, technical, or material support (i.e., reporting or organizing data, constructing databases): J.A. Kelber, T. Wright, R.L. Klemke
Study supervision: J.A. Kelber, R.L. Klemke

Introduction

Pancreatic ductal adenocarcinoma (PDAC) is the fourth leading cause of cancer-related death. Newly diagnosed patients with PDACs have a median survival of less than 1 year and a 5-year survival rate of 3% to 5% (1, 2). While oncogenic KRas is the initiating mutation in nearly all PDACs, the development of effective therapies targeting this GTPase or downstream effectors has shown little promise in fighting this disease to date (1–3). Therefore, functional biomarkers that can identify early onset of PDAC and that may be viable therapeutic targets are highly sought after (1, 2).

In addition to activating mutations in the KRas oncogene, more than 60% of PDACs have elevated Src activity (4) and overexpress ErbB2 (3). Thus, therapeutic targeting of Src or ErbB2 may be promising for the majority of patients. However, there have been a limited number of studies testing this hypothesis, and these have not been conclusive (4–9). This may be due to the combined effects of multiple oncogenic pathways contributing to disease progression in PDAC, or there may be unidentified molecular regulators that induce therapy-resistant phenotypes (10, 11).

We recently identified PEAK1 (pseudopodium-enriched atypical kinase one, SGK269) as a catalytically active non-receptor tyrosine kinase that associates with the cytoskeleton and regulates cell migration and proliferation (12). Tyrosine kinases are important candidates as biomarkers and therapeutic targets because they induce specific phosphorylation signatures and their catalytic activity and downstream signals can be inhibited by small molecules (13). The goal of this current study was to assess the role of PEAK1 expression as a diagnostic/prognostic biomarker and potential therapeutic target in human malignancies. In this regard, we show that PEAK1 upregulation occurs in multiple human malignancies (including PDAC), PEAK1 is necessary for PDAC growth and metastasis *in vivo*, KRas induces PEAK1-dependent Src/PEAK1/ErbB2 signaling, and that PEAK1 is an oncogenic rheostat, which balances Src activity to promote PDAC therapy resistance.

Materials and Methods

Cell lines, DNA/lentiviral constructs, and reagents

Details about cell lines and culture conditions are given in the Supplementary Materials and Methods. shCntrl and shPEAK1 (FG12 vector) constructs have been previously published (12). The shPEAK1 [3′ untranslated region (UTR)] and shErbB2 (pLK0.1 vector) constructs were purchased from Open Biosystems/The RNAi Consortium (Thermo Scientific). Control, PEAK1, and ErbB2 shRNA sequences and details about lentiviral production are given in the Supplementary Materials and Methods. Short hairpin RNA (shRNA)/siRNA pools (containing at least 4 unique siRNA sequences each) against KRas (Santa Cruz Biotechnology, shRNA lentivirus particles) and Src (Dharmacon, siRNA transient transfection) were purchased along with the appropriate nontargeting control siRNAs. GFP-vector, GFP-PEAK1, and GFP-PEAK1 mutants have been previously described (12). For stable over-expression of PEAK1 and 3′UTR shRNA rescue experiments, human PEAK1 was subcloned into the pCSC-SP-PW-GFP lentiviral vector (Addgene) with *Eco*RI and *Kpn*I sites and transduced cells were sorted for GFP. Empty vector and NeuT constructs (pBabe-puro vector) have been previously described and were used with the appropriate packaging DNAs to generate retroviral particles for cell transduction (14). Details about antibodies, inhibitors, and other reagents are given in the Supplementary Materials and Methods. Trastuzumab was provided by Genentech under MTA agreement #210708.

Oncomine analysis

Normalized PEAK1, Src, or ErbB2 expression data and *P* values were downloaded from Oncomine (Compendia Bioscience). Citations for individual studies are included in the Supplementary Data. Heatmaps were generated by Excel. Gene expression levels were plotted with Tukey or average ± SEM analyses for each patient group.

Immunohistochemistry

Human pancreatic cancer tissue array was purchased from US Biomax, Inc. PDX-1-Cre:LSL-KRAS^{G12D} mouse pancreas sections were kindly provided by A.M. Lowy. Samples from patients BK-13 and BK-14 were collected and processed as described later in accordance with UCSD (La Jolla, CA) Institutional Review Board (IRB) #071136X. PEAK1 protein expression was determined with the standard avidin-biotin immunoperoxidase procedures, sodium citrate antigen retrieval methods, and the VECTASTAIN Elite ABC Kit from Vector Laboratories according to the manufacturer's protocol. Mouse monoclonal anti-SGK269 and rabbit polyclonal anti-PEAK1 were purchased from Santa Cruz Biotechnology and Millipore, respectively, and used at a 1:200 dilution. Anti-ErbB2 (29D8) and anti-Src (36D10) antibodies were purchased from Cell Signaling and used according to manufacturer's recommendations. Images were collected with a Leica DM2500 microscope.

Mouse strains

The PDX-1-Cre:LSL-KRAS^{G12D} transgenic murine model was previously described (15).

Patient sample collection and preparation

In accordance with IRB #071136X (M. Bouvet), fresh tumor specimens from patients undergoing routine cancer surgery were collected in cold RPMI for subsequent PCR and immunohistochemical preparation and analysis. All patient identification information was removed and all samples were made anonymous. Patients signed an informed consent document before their operative procedure, which acknowledged that a portion of the resected tissue would be used for research.

RT-PCR and quantitative PCR

mRNA extraction, purification, DNA synthesis, and reverse trascription (RT) or quantitative (qPCR) primers used are described in the Supplementary Materials and Methods. All qPCR data were processed with the relative quantification method and plotted as average fold change (±SEM, unless otherwise indicated) in relation to normal tissue, appropriate untreated, vehicle-treated, or shRNA controls.

CyQUANT direct cell proliferation assay

Analysis of cell growth was conducted according to manufacturer's protocol (Invitrogen). Briefly, cells were plated in triplicate into 96-well plates at a density of 200 to 500 cells per well in complete media. Twenty-four hours later, cell media were changed to 2% serum-containing media and left untreated or treated with indicated reagents. Viable cell number was measured on days 3 or 8 based upon CyQuant Green fluorescence emission at 525 nm.

Three-dimensional spheroid assay

Analysis of three-dimensional (3D) tumorsphere growth was conducted as previously described (16). Briefly, cells were plated into Dulbecco's Modified Eagle's Medium (DMEM): F12 (1:1) containing B27 supplement, 10 μg/mL basic fibroblast growth factor, 10 μg/mL EGF, and 4 μg/mL heparin sulfate. Cells were grown for 14 to 21 days and spheroids were imaged with a wide-field light microscope.

Soft agar transformation experiments

Analysis of anchorage-independent cell growth was conducted according to the manufacturers' protocol (Cell Biolabs). Briefly, 96-well plates were prepared with 50 μL per well surface layers consisting of 0.6% agar resuspended in cell culture media. An additional 75 μL per well of 0.33% agar cell culture media containing 5,000 cells was then added to each well, followed by the addition of 50 μL of cell culture media. Brightfield microscope images were collected at ×10 magnification with a Nikon TE instrument and colonies were resuspended and quantified with Cell Biolabs' CyQuant Green fluorescent dye at 525 nm.

Orthotopic implantation experiments

Protocols were followed as previously described (17). Details are given in the Supplementary Materials and Methods section. For survival analysis, animal health was assessed 3 times per week and animals were sacrificed when they reached a pre-defined state of premorbidity (i.e., >3 cm tumor diameter and one of the following: impaired movement, cachexia, or observable ascites accumulation; or impaired movement, cachexia, and observable ascites accumulation). Kaplan–Meier curves were plotted for each animal group, and statistical analysis was conducted with Prism software (GraphPad). Details of sample processing are given in the Supplementary Materials and Methods.

Chicken embryo metastasis assay

Fertilized chicken eggs were purchased from McIntire Poultry and incubated for 14 days (37°C, 100% humidity). A 1-cm^2 square window was created in the eggshell to expose the underlying vasculature. Tumor cells were suspended in sterile PBS at a concentration of 3×10^6/mL and 3×10^5 tumor cells were injected into one of the chorioallantoic membrane (CAM) veins. After incubating embryos for another 48 hours, Rhodamine-lectin (Vector Biolabs, 100 μL per chick, 0.5mg/mL) was injected into the CAM vein. Following appropriate euthanizing procedures, the chicken brain and liver were removed and imaged with either a Leica MZFLIII microscope (×1.25) or a Nikon c1-si confocal microscope (×10–60).

Immunoprecipitation and Western blotting

All immunoprecipitations and Western blotting were conducted as previously described (12).

Confocal microscopy

Imaging and processing were conducted as described in Supplementary Materials and Methods.

Statistical analysis

All quantified data were plotted and analyzed in GraphPad Prism 5.0 with ANOVA, Student *t* test, nonlinear regression analysis, or Kaplan–Meier curve analysis. Data are representative of at least 3 independent experiments and are reported as replicate averages ± SEM, unless otherwise indicated. *, **, or *** represent *P* values < 0.05, 0.01, or 0.001, respectively, unless otherwise noted.

Results

PEAK1 is overexpressed in multiple human malignancies and is an early biomarker for PDAC development and progression

Because it is not known whether oncogenic transformation regulates PEAK1 expression or whether PEAK1 contributes widely to human malignancies, we first sought to determine the expression profile of PEAK1 in various human cancers in comparison with normal tissues. PEAK1 expression is significantly upregulated in multiple human tumors in comparison with normal tissues (Fig. 1A) and shows a strong correlation with various subcategories of these cancers that are associated with poor disease prognosis (Supplementary Table S1). No significant changes in PEAK1 mRNA levels were observed between normal and malignant tissues for bladder, head and neck, lung, sarcoma, and melanoma tumors. Because the mortality and incidence for PDAC are almost equal due to few diagnostic biomarkers and therapeutic targets, we focused our subsequent PEAK1 expression analyses on this disease. We examined changes in PEAK1 protein levels in human PDAC patient tissue arrays and a murine model of KRas-induced PanIN (PDX-1-Cre:LSL-KRAS^{G12D}; ref. 15). PEAK1 protein expression was increased in PDAC tissues in comparison with normal tissues and correlated with grade (Fig. 1B). Furthermore, we observed that PEAK1 expression was elevated in PanIN lesions (Fig. 1C and Supplementary Table S1), showing that PEAK1 represents an early biomarker for pancreatic ductal neoplasia (1, 18).

KRas induces Src-dependent PEAK1 expression in PDAC and other human malignancies

While the above findings suggest that PEAK1 is deregulated during oncogenic reprogramming, the mechanism driving PEAK1 upregulation remains unclear. Because PanIN and PDAC progression are nearly always associated with activating mutations in the KRas oncogene and because PEAK1 is upregulated in PanIN tissues from PDX-1-Cre:LSL-KRAS^{G12D} mice, we tested whether PEAK1 expression correlated with oncogenic Ras mutations in human cancers. RT-PCR, qPCR, and immunohistochemical analyses of normal pancreas and oncogenic KRas-positive PDAC tissues collected from patients BK-13 and BK-14 after surgical resection showed that PEAK1 is overexpressed in PDAC tissue in conjunction with the presence of the G12D oncogenic KRas mutant (Fig. 2A and B and Supplementary Fig. S1A). Furthermore, human cancers positive for oncogenic *KRas* or *NRas* mutations (Fig. 2C) or HRas-transformed breast epithelial cells (Supplementary Table S1) showed a significant increase in PEAK1 expression. In agreement with these data, introduction of constitutively active KRas^{G12D} into human pancreatic nestin-expressing (HPNE; refs.11, 19) cells or KRas knockdown in established PDAC cell lines robustly increased or decreased, respectively, PEAK1 protein and mRNA levels (Fig. 2D and Supplementary Fig. S1B).

We subsequently sought to identify the pathway downstream of KRas that induces PEAK1 expression. Pharmacologic inhibition of phosphoinositide 3-kinase (PI3K), mitogen-activated protein (MAP)/ERK kinase (MEK), or Src in HPNE-KRas and PANC1 cells revealed that PEAK1 expression is dependent upon Src-mediated transcriptional regulation (Fig. 2E and Supplementary Fig. S1C, S1D, and S1F). Importantly, suppression of Src kinase in these cells via RNA interference (RNAi) also reduced PEAK1 expression (Supplementary Fig. S1E). Taken together, these findings show that PEAK1 protein expression is positively regulated by KRas/Src signaling in human malignancies and human PDAC primary samples and cell lines.

PEAK1 is necessary for KRas-induced anchorage-dependent and -independent expansion of pancreatic cancer cells

Consistent with the role of KRas in driving PEAK1 expression, PEAK1 was necessary and sufficient for KRas-induced anchorage-dependent expansion in HPNE cells (Fig. 3A and B and Supplementary Fig. S2A and S2B). Importantly, overexpression of wild-type PEAK1 or a C-terminal truncation mutant (C1) containing the kinase domain was sufficient to induce HPNE cell expansion under anchorage-dependent conditions. Mutational inactivation of the ATP-binding site abrogated this effect, showing that PEAK1 kinase activity (12) is critical for its effect in these assays (Fig. 3C and Supplementary Fig. S2C). Conversely, depletion of KRas or PEAK1 from FG and PANC1 PDAC cell lines (Fig. 2D and Supplementary Fig. S2A) inhibited anchorage-dependent cell expansion (Fig. 3D). In addition, we discovered that PEAK1 is essential for KRas-induced formation and expansion of 3D tumorspheres (Fig. 3E and Supplementary Fig. S2D), which is an *in vitro* measure of tumor-initiating potential (16). We further analyzed the ability of PEAK1 overexpression and knockdown to modulate HPNE cell transformation, as analyzed by anchorage-independent growth. As shown in Fig. 3F, HPNE-KRas cells overexpressing PEAK1 formed more colonies in soft agar, and these colonies were also larger. PEAK1 knockdown significantly reduced the ability of HPNE-KRas cells to grow under these conditions. Importantly, this effect was rescued by overexpressing PEAK1.

PEAK1 is necessary for tumor formation, progression, and metastasis *in vivo*

The above results strongly suggested that PEAK1 might regulate pancreatic cancer growth *in vivo*. Therefore, we next investigated whether altering PEAK1 expression could interfere with PDAC tumor formation and metastasis *in vivo*. In these studies, FG cells were measured for their ability to form tumors and metastasize with a preclinical orthotopic implantation mouse model of PDACs (Fig. 4A; refs. 17, 20). PEAK1 knockdown significantly reduced tumor formation (Fig. 4B and Supplementary Fig. S3A and S3B), whereas PEAK1 overexpression caused a significant increase in tumorigenesis *in vivo* (Supplementary Fig. S3C–S3E). Furthermore, PEAK1 knockdown suppressed metastasis to multiple sites and increased animal survival compared with animals implanted with control cells expressing PEAK1 (Fig. 4C and D and Supplementary Fig. S3F). Notably, the median survival of control animals was 64 days, whereas median survival of the PEAK1-depleted group was 97 days ($P = 0.0022$; Fig. 4D). In support of these data, depletion of PEAK1 in HPNE-KRas^{G12D} cells abrogated liver and brain metastasis (Fig. 4E and Supplementary Fig. S3G) in the chicken embryo (21). These data are also consistent with our observations that PEAK1 levels are significantly increased in the highly metastatic FGM cell line derived from FG cells (Supplementary Fig. S3H) and in metastatic foci originating from human PDAC and other cancers in comparison with the primary tumor of origin (Fig. 4F, Supplementary Fig. S3I and Table S1; ref. 22). Together, these data show an essential role for PEAK1 during PDAC growth and metastasis *in vivo*.

Suppression of ErbB2 in PDAC cells drives PEAK1-dependent tumor formation *in vivo*

Similar to PEAK1, both ErbB2 and Src are upregulated in human PDAC downstream of oncogenic KRas (Fig. 5A and B and Supplementary Fig. S4A–S4E; refs. 23–25). While Src is known to cooperate with KRas during pancreatic neoplasia (4), the role of ErbB2 in PDAC remains unclear (1, 2). For these reasons, we initially sought to determine whether there was a functional relationship between the coinduction of PEAK1 and ErbB2 tyrosine kinases in PDACs. Surprisingly, silencing ErbB2 (Supplementary Fig. S4F) in FG cells significantly increased orthotopic tumor formation in mice (Fig. 5C and Supplementary Fig. S4G). Notably, this response was associated with increased PEAK1 expression *in vivo* (Fig. 5D) and *in vitro* (Fig. 5E and Supplementary Fig. S4H), suggesting that PEAK1 upregulation compensated for the loss of ErbB2 to drive tumor formation. Indeed, silencing

PEAK1 in ErbB2-depleted FG cells fully abrogated tumor formation beyond that of PEAK1 knockdown alone (Fig. 5C–E and Supplementary Fig. S4G and S4H). These findings are also consistent with our data showing that PEAK1 overexpression in FG cells increases tumor formation (Supplementary Fig. S3C–S3E). These data show that ErbB2 suppression in PDAC cells potentiates tumor formation by upregulating PEAK1 protein levels. Interestingly, overexpression of a constitutively active form of ErbB2 (NeuT) in FG cells did not alter PEAK1 expression or the tumorigenic potential of these cells *in vivo* (Supplementary Fig. S4I–S4L). This result suggests that ErbB2 is a permissive factor in PDACs and that oncogenic programs active in this disease are selectively sensitive to decreased ErbB2 levels.

PEAK1 modulates Src and ErbB2 kinase activities and complex assembly

PEAK1 knockdown inhibited ErbB2 kinase activity as indicated by decreased phosphorylation of Y1248 and Y877 (Fig. 5E and Supplementary Fig. S4H; refs. 26, 27). ErbB2-Y877 is a reported Src substrate site that potentiates ErbB2 autophosphorylation on other tyrosine residues such as Y1248 and enhances its transforming potential (26). Therefore, these findings suggest that PEAK1 can regulate Src activity toward ErbB2 to modulate its kinase activity. In this regard, PEAK1 knockdown potently inhibited Src kinase activity and the assembly of an active Src/ErbB2 kinase complex (Fig. 5E and F and Supplementary Fig. S4H). Furthermore, active Src and ErbB2 co-precipitated with PEAK1 from PDAC cell lysates indicating that all 3 proteins participate in a molecular complex (Fig. 5F and Supplementary Fig. S4M). Because KRas induces PEAK1 expression in a Src-dependent manner (Fig. 2E and Supplementary Fig. S1C–S1F), we further hypothesized that PEAK1 upregulation following ErbB2 depletion may also occur via an Src-dependent mechanism. Pharmacologic or RNAi inhibition of Src in FG cells with and without ErbB2 suppressed PEAK1 expression at both the transcript and protein levels (Fig. 5G and H). Taken together, our findings show that KRas activation induces the upregulation of Src, PEAK1, and ErbB2 to form a feed-forward, self-sustaining tyrosine kinase amplification loop that promotes PDAC growth and metastasis.

Src/PEAK1/ErbB2 signaling drives trastuzumab and gemcitabine resistance in pancreatic cancer cells

Because Src and ErbB2 inhibitors are currently in clinical trials for pancreatic cancer and we have shown that inhibition of Src activity and ErbB2 expression modulate PEAK1 protein levels, we sought to determine whether Src (dasatinib) or ErbB2 (trastuzumab) inhibition might elicit compensatory expression of *PEAK1*, *Src*, and/or *ErbB2* genes. Importantly, inhibition of PEAK1 expression did not induce compensatory transcription of Src or ErbB2 (Fig. 6A). In contrast, whereas dasatinib inhibited PEAK1 expression, it significantly increased transcription of both ErbB2 and Src (Fig. 6A, middle and right). This compensatory upregulation of ErbB2 in response to dasatinib may have important clinical implications. However, we show here that increased ErbB2 activity above endogenous levels in PDAC cells does not promote increased tumor growth (Supplementary Fig. S4I–S4L). Therefore, as dasatinib potently blocks both Src activity and PEAK1 expression, even in the context of upregulated ErbB2, it is likely that this therapeutic approach will provide some benefit to patients (4, 9). On the other hand, directly inhibiting ErbB2 expression and function with trastuzumab alone may not be a viable therapeutic option because it induced PEAK1 expression (Fig. 6A, left, and 6B), which in turn, can drive Src activity and PDAC growth (Figs. 5C–E and 6B, and Supplementary Fig. S4G and S4H). Taken together, these data suggest that targeting PEAK1 may be a preferred method for treating PDAC as it minimizes compensatory signaling through Src and ErbB2 kinases.

The above results do suggest that dual inhibition of both ErbB2 and PEAK1 may further overcome trastuzumab resistance in PDAC preclinical and clinical studies. Trastuzumab (Herceptin, Genentech Inc.) acts to cause internalization, degradation, and inactivation of the ErbB2 receptor (28) and is currently being evaluated in combination with gemcitabine, which is the standard chemotherapy given to patients with PDAC. However, studies to date suggest that trastuzumab offers little benefit alone or in combination with gemcitabine (2, 6, 7, 29). These data, combined with the fact that PEAK1 is upregulated in trastuzumab-resistant PDAC cell lines and patients with amplified ErbB2 levels (Supplementary Fig. S5A and S5B), led us to investigate whether the ineffectiveness of trastuzumab-based therapies could be because of a PEAK1/ Src compensation mechanism following ErbB2 suppression. Consistent with shRNA knockdown of ErbB2 in FG cells, trastuzumab treatment of PANC1 cells (a trastuzumab-resistant line; ref. 6) reduced ErbB2 expression significantly and increased PEAK1 expression, Src activity, and robust Y877 phosphorylation of the residual ErbB2 protein (Fig. 6B). PEAK1 knockdown abrogated this effect (Fig. 6B) and greatly sensitized these cells to trastuzumab (Fig. 6C). While overexpression of PEAK1 in HPNE-KRas cells did not significantly change their response to trastuzumab, PEAK1 knockdown enabled trastuzumab to elicit growth-inhibitory effects under anchorage-dependent conditions (Fig. 6D). Rescuing PEAK1 expression in the HPNE-KRas cells reversed this effect, causing these cells to regain their trastuzumab-resistant phenotype (Fig. 6D). Furthermore, PEAK1 knockdown reduced the IC_{50} values of trastuzumab (Fig. 6E) and a commercially available ErbB2-targeting antibody (Supplementary Fig. S5C) by approximately 100- and 10-fold, respectively, whereas PEAK1 overexpression in FG cells made them nonresponsive to trastuzumab *in vitro* (Supplementary Fig. S5D). These findings support a mechanism by which elevated PEAK1/Src signaling compensates for loss of ErbB2 function in PDAC and, therefore, contributes to resistance of ErbB2-targeted therapies.

As mentioned earlier, the standard therapy regimen for patients with metastatic pancreatic cancer is gemcitabine. However, most patients with advanced metastatic disease show little response to this treatment (1, 30). Because Src activity has recently been identified as a contributing factor to gemcitabine resistance in pancreatic cancer (9) and we show that Src inhibition with dasatinib sensitized FG cells to gemcitabine (Supplementary Fig. S5E), we reasoned that PEAK1 suppression may also sensitize PDAC cells to growth inhibition by gemcitabine treatment. In this regard, shPEAK1 FG cells were 10 times more sensitive to gemcitabine treatment *in vitro* than in control cells (Fig. 6F). In agreement with these data, previous studies have shown a significant increase in PEAK1 expression in patients with lung cancer who are resistant to gemcitabine treatment (Supplementary Fig. S5F and Table S1). Taken together with our earlier results showing that PEAK1 mediates the formation and function of a triple-kinase complex between Src, PEAK1, and ErbB2 to promote PDAC progression, these findings suggest that the development of combination therapies that include PEAK1 inhibition or suppression may provide maximum benefit for patients.

Discussion

We originally identified PEAK1 as a tyrosine phosphorylated protein enriched in the pseudopodium of migrating cells (12, 31). PEAK1 localizes to integrin-mediated focal adhesions and actin stress fibers, where it regulates the cytoskeleton and shape changes necessary for cell migration. Here, we report that PEAK1 also regulates cancer cell growth and progression. Although it is not yet known how PEAK1 regulates cancer growth and cancer cell motility, PEAK1 can receive input signals from integrin adhesions and growth factor receptors, which send vital proliferation, survival, and motility information from the surrounding extracellular environment to the cell's interior (32–34). In this regard, we have previously shown that growth factors promote PEAK1 tyrosine phosphorylation in a Src-

dependent manner (12, 31). Also, PEAK1 overexpression in cancer cells is sufficient to promote extracellular signal–regulated kinase (ERK) activation and phosphorylation of the focal adhesion proteins p130CAS and paxillin (12, 31). Together, these findings suggest that PEAK1 is an important cytoskeletal regulator that controls cancer cell growth and migration.

PEAK1 is upregulated in many solid tumors and blood-born cancers (Fig. 1A and Supplementary Table S1). This suggests that PEAK1 plays fundamental roles in tumor progression downstream of the diverse oncogenic insults found in human malignancies. While the precise role of PEAK1 in these malignancies needs to be defined further, we show here that in PDACs, activating mutations in the *KRas* oncogene drive the aberrant upregulation of PEAK1 via Src-dependent transcriptional regulation. This can affect cancer progression in 2 ways. First, PEAK1 upregulation increases Src kinase activity above that already induced by KRas activation (Fig. 5E and Supplementary Fig. S4H). PEAK1 has a highly conserved Src consensus phosphorylation site and Src SH2–binding domain at Y665. Thus, it is possible that KRas drives the initial Src activity that promotes both increased PEAK1 protein expression and the phosphorylation of Y665. We suspect that this increases Src binding to PEAK1-Y665 via its SH2 domain, which in turn stabilizes Src in the open kinase-active conformation, and further promotes tumorigenesis (ref. 35; Supplementary Fig. S6).

Second, PEAK1 mediates Src/ErbB2 binding and ErbB2 phosphorylation at Y877 (Fig. 5E and F and Supplementary Fig. S4H and S4M). Phosphorylation of ErbB2-Y877 is Src-dependent and can enhance the oncogenic potential of ErbB2 (26). Therefore, it is possible that enhanced ErbB2 activation, by PEAK1/Src signaling, can also contribute to cancer growth and progression (Supplementary Fig. S6). If this is the case, depletion of ErbB2 should reduce tumorigenesis. Surprisingly though, depletion of ErbB2 protein from PDAC cells enhanced tumorigenesis in a PEAK1/Src-dependent fashion (Fig. 5C–E and Supplementary Fig. S4G and S4H). Furthermore, overexpression of the constitutively active NeuT receptor did not modulate PEAK1 expression or increase tumor growth (Supplementary Fig. S4I–S4L). This suggests that elevating ErbB2 activation above endogenous levels in pancreatic cancer cells does not further contribute to tumor growth and that ErbB2 overexpression is permissive during later stages of PDACs (36). Interestingly, it has been previously reported that oncogenes known to contribute to tumorigenesis in some tumor types have no phenotype when overexpressed in other cancers (37, 38). Furthermore, it will be important that future studies investigate the role of ErbB2 during early pancreatic neoplasia. One explanation of these results is that the loss of ErbB2 protein from the PEAK1/Src kinase complex makes this active complex available to target new substrates (such as other growth factor receptors or intracellular effector molecules) that can also drive cancer. Alternatively, ErbB2 inactivation could inhibit an unidentified negative feedback pathway that normally permits or holds PEAK1/Src activity in check within tumor cells. In this regard, we show that ErbB2 suppression via RNAi or trastuzumab increases PEAK1 expression and Src signaling, leading to sustained phosphorylation of the residual ErbB2 protein (Figs. 5E–H and 6A and Supplementary Fig. S4H). Yet, it is still possible that other feedback mechanisms are in action, and the specific protumorigenic mechanism(s) of PEAK1/Src hyperactivation downstream of ErbB2 inactivation as well as the role of PEAK1 in other cancers need to be further elucidated. In any case, our findings clearly show that PEAK1 is necessary for PDAC progression whether or not ErbB2 is present.

Because our data suggest that ErbB2 plays a permissive, oncogene-sensing role in PDAC, our findings that trastuzumab resistance results from compensatory PEAK1/Src signaling have important implications for this disease. The therapeutic effectiveness of trastuzumab is currently being tested in human PDAC clinical trials in combination with gemcitabine (2, 6, 7, 29). However, the majority of patients show no benefit from trastuzumab treatment. Thus,

our finding that PEAK1/Src signaling can compensate for the loss of ErbB2 activity may provide a plausible explanation for the poor clinical response to trastuzumab and are in agreement with previous studies. In our studies, trastuzumab initiated compensatory PEAK1-dependent signaling (Fig. 6A–E and Supplementary Fig. S5A–S5D). Thus, PEAK1 may be a preferred target against which novel therapies can be developed for patients with PDACs, either alone or in combination with existing therapies. Finally, PEAK1 inhibition sensitized PDAC cells to gemcitabine treatment (Fig. 6F). Because gemcitabine represents the standard of care for patients with PDAC, therapeutic interventions that target PEAK1 may improve patient outcome in combination with gemcitabine therapy.

In summary, KRas-induced PEAK1 mediates pancreatic cancer growth, metastasis, and therapy resistance via activation of Src kinase. While many factors contribute to the pathogenesis of PDACs, a detailed understanding of the molecular components, such as PEAK1, that can drive cancer progression, metastasis, and therapy resistance may lead to new avenues for disease diagnosis and treatment.

Supplementary Material

Refer to Web version on PubMed Central for supplementary material.

Acknowledgments

The authors thank members of the Klemke, Bouvet, and Lowy laboratories and Dr. Peter Gray for instructive feedback and discussions about the manuscript. The authors thank Dr. Cynthia Snyder who assisted with the histopathology analysis of tumor sections. The authors also thank Elizabeth Hampton, Ryan Matson, and Tiffany Taylor for assistance with molecular biology and cell culture protocols.

Grant Support

This work was supported by the NIH-IRACDA (NIH - Institutional Research and Academic Career Development Award) Postdoctoral Fellowship GM06852 (J.A. Kelber) and NIH grants CA097022 and CA129231 (R.L. Klemke), CA132971 (M. Bouvet) and CA137692 (A.M. Lowy).

References

1. Hezel AF, Kimmelman AC, Stanger BZ, Bardeesy N, Depinho RA. Genetics and biology of pancreatic ductal adenocarcinoma. Genes Dev. 2006; 20:1218–49. [PubMed: 16702400]
2. Kern SE, Shi C, Hruban RH. The complexity of pancreatic ductal cancers and multidimensional strategies for therapeutic targeting. J Pathol. 2011; 223:295–306. [PubMed: 21125682]
3. Ghaneh P, Costello E, Neoptolemos JP. Biology and management of pancreatic cancer. Gut. 2007; 56:1134–52. [PubMed: 17625148]
4. Shields DJ, Murphy EA, Desgrosellier JS, Mielgo A, Lau SK, Barnes LA, et al. Oncogenic Ras/Src cooperativity in pancreatic neoplasia. Oncogene. 2011; 30:2123–34. [PubMed: 21242978]
5. Larbouret C, Robert B, Navarro-Teulon I, Thezenas S, Ladjemi MZ, Morisseau S, et al. *In vivo* therapeutic synergism of anti-epidermal growth factor receptor and anti-HER2 monoclonal antibodies against pancreatic carcinomas. Clin Cancer Res. 2007; 13:3356–62. [PubMed: 17545543]
6. Kimura K, Sawada T, Komatsu M, Inoue M, Muguruma K, Nishihara T, et al. Antitumor effect of trastuzumab for pancreatic cancer with high HER-2 expression and enhancement of effect by combined therapy with gemcitabine. Clin Cancer Res. 2006; 12:4925–32. [PubMed: 16914581]
7. Pratesi G, Petrangolini G, Tortoreto M, Addis A, Zunino F, Calcaterra C, et al. Antitumor efficacy of trastuzumab in nude mice orthotopically xenografted with human pancreatic tumor cells expressing low levels of HER-2/neu. J Immunother. 2008; 31:537–44. [PubMed: 18528301]
8. Buchler P, Reber HA, Buchler MC, Roth MA, Buchler MW, Friess H, et al. Therapy for pancreatic cancer with a recombinant humanized anti-HER2 antibody (herceptin). J Gastrointest Surg. 2001; 5:139–46. [PubMed: 11331475]

9. Nagaraj NS, Washington MK, Merchant NB. Combined blockade of Src kinase and epidermal growth factor receptor with gemcitabine overcomes STAT3-mediated resistance of inhibition of pancreatic tumor growth. Clin Cancer Res. 2011; 17:483–93. [PubMed: 21266529]
10. Fleming JB, Shen GL, Holloway SE, Davis M, Brekken RA. Molecular consequences of silencing mutant K-ras in pancreatic cancer cells: justification for K-ras-directed therapy. Mol Cancer Res. 2005; 3:413–23. [PubMed: 16046552]
11. Zhao S, Wang Y, Cao L, Ouellette MM, Freeman JW. Expression of oncogenic K-ras and loss of Smad4 cooperate to induce the expression of EGFR and to promote invasion of immortalized human pancreas ductal cells. Int J Cancer. 2010; 127:2076–87. [PubMed: 20473902]
12. Wang Y, Kelber JA, Tran Cao HS, Cantin GT, Lin R, Wang W, et al. Pseudopodium-enriched atypical kinase 1 regulates the cytoskeleton and cancer progression [corrected]. Proc Natl Acad Sci U S A. 2010; 107:10920–5. [PubMed: 20534451]
13. Manning G, Whyte DB, Martinez R, Hunter T, Sudarsanam S. The protein kinase complement of the human genome. Science. 2002; 298:1912–34. [PubMed: 12471243]
14. Brandt R, Wong AM, Hynes NE. Mammary glands reconstituted with Neu/ErbB2 transformed HC11 cells provide a novel orthotopic tumor model for testing anti-cancer agents. Oncogene. 2001; 20:5459–65. [PubMed: 11571643]
15. Hingorani SR, Petricoin EF, Maitra A, Rajapakse V, King C, Jacobetz MA, et al. Preinvasive and invasive ductal pancreatic cancer and its early detection in the mouse. Cancer Cell. 2003; 4:437–50. [PubMed: 14706336]
16. Hermann PC, Huber SL, Herrler T, Aicher A, Ellwart JW, Guba M, et al. Distinct populations of cancer stem cells determine tumor growth and metastatic activity in human pancreatic cancer. Cell Stem Cell. 2007; 1:313–23. [PubMed: 18371365]
17. Snyder CS, Kaushal S, Kono Y, Cao HS, Hoffman RM, Bouvet M. Complementarity of ultrasound and fluorescence imaging in an orthotopic mouse model of pancreatic cancer. BMC Cancer. 2009; 9:106. [PubMed: 19351417]
18. Harsha HC, Kandasamy K, Ranganathan P, Rani S, Ramabadran S, Gollapudi S, et al. A compendium of potential biomarkers of pancreatic cancer. PLoS Med. 2009; 6:e1000046. [PubMed: 19360088]
19. Carriere C, Seeley ES, Goetze T, Longnecker DS, Korc M. The Nestin progenitor lineage is the compartment of origin for pancreatic intraepithelial neoplasia. Proc Natl Acad Sci U S A. 2007; 104:4437–42. [PubMed: 17360542]
20. Hoffman RM. The multiple uses of fluorescent proteins to visualize cancer *in vivo*. Nat Rev Cancer. 2005; 5:796–806. [PubMed: 16195751]
21. Deryugina EI, Quigley JP. Chick embryo chorioallantoic membrane model systems to study and visualize human tumor cell metastasis. Histochem Cell Biol. 2008; 130:1119–30. [PubMed: 19005674]
22. Harada T, Chelala C, Bhakta V, Chaplin T, Caulee K, Baril P, et al. Genome-wide DNA copy number analysis in pancreatic cancer using high-density single nucleotide polymorphism arrays. Oncogene. 2008; 27:1951–60. [PubMed: 17952125]
23. Badea L, Herlea V, Dima SO, Dumitrascu T, Popescu I. Combined gene expression analysis of whole-tissue and microdissected pancreatic ductal adenocarcinoma identifies genes specifically over-expressed in tumor epithelia. Hepatogastroenterology. 2008; 55:2016–27. [PubMed: 19260470]
24. Day JD, Digiuseppe JA, Yeo C, Lai-Goldman M, Anderson SM, Goodman SN, et al. Immunohistochemical evaluation of HER-2/neu expression in pancreatic adenocarcinoma and pancreatic intraepithelial neoplasms. Hum Pathol. 1996; 27:119–24. [PubMed: 8617452]
25. Lutz MP, Esser IB, Flossmann-Kast BB, Vogelmann R, Luhrs H, Friess H, et al. Overexpression and activation of the tyrosine kinase Src in human pancreatic carcinoma. Biochem Biophys Res Commun. 1998; 243:503–8. [PubMed: 9480838]
26. Marcotte R, Zhou L, Kim H, Roskelly CD, Muller WJ. c-Src associates with ErbB2 through an interaction between catalytic domains and confers enhanced transforming potential. Mol Cell Biol. 2009; 29:5858–71. [PubMed: 19704002]

27. Muthuswamy SK, Gilman M, Brugge JS. Controlled dimerization of ErbB receptors provides evidence for differential signaling by homo- and heterodimers. Mol Cell Biol. 1999; 19:6845–57. [PubMed: 10490623]

28. Kruser TJ, Wheeler DL. Mechanisms of resistance to HER family targeting antibodies. Exp Cell Res. 2010; 316:1083–100. [PubMed: 20064507]

29. Safran H, Iannitti D, Ramanathan R, Schwartz JD, Steinhoff M, Nauman C, et al. Herceptin and gemcitabine for metastatic pancreatic cancers that overexpress HER-2/neu. Cancer Invest. 2004; 22:706–12. [PubMed: 15581051]

30. Collisson EA, Sadanandam A, Olson P, Gibb WJ, Truitt M, Gu S, et al. Subtypes of pancreatic ductal adenocarcinoma and their differing responses to therapy. Nat Med. 2011; 17:500–3. [PubMed: 21460848]

31. Kelber JA, Klemke RL. PEAK1, a novel kinase target in the fight against cancer. Oncotarget. 2010; 1:219–23. [PubMed: 21301050]

32. Ridley AJ. Life at the leading edge. Cell. 2011; 145:1012–22. [PubMed: 21703446]

33. Rathinam R, Berrier A, Alahari SK. Role of Rho GTPases and their regulators in cancer progression. Front Biosci. 2011; 17:2561–71. [PubMed: 21622195]

34. Linding R, Jensen LJ, Pasculescu A, Olhovsky M, Colwill K, Bork P, et al. NetworKIN: a resource for exploring cellular phosphorylation networks. Nucleic Acids Res. 2008; 36:D695–9. [PubMed: 17981841]

35. Lu XL, Cao X, Liu XY, Jiao BH. Recent progress of Src SH2 and SH3 inhibitors as anticancer agents. Curr Med Chem. 2010; 17:1117–24. [PubMed: 20158477]

36. Bardeesy N, DePinho RA. Pancreatic cancer biology and genetics. Nat Rev Cancer. 2002; 2:897–909. [PubMed: 12459728]

37. Haigis KM, Kendall KR, Wang Y, Cheung A, Haigis MC, Glickman JN, et al. Differential effects of oncogenic K-Ras and N-Ras on proliferation, differentiation and tumor progression in the colon. Nat Genet. 2008; 40:600–8. [PubMed: 18372904]

38. Hann A, Gruner A, Chen Y, Gress TM, Buchholz M. Comprehensive analysis of cellular galectin-3 reveals no consistent oncogenic function in pancreatic cancer cells. PLoS One. 2011; 6:e20859. [PubMed: 21698183]

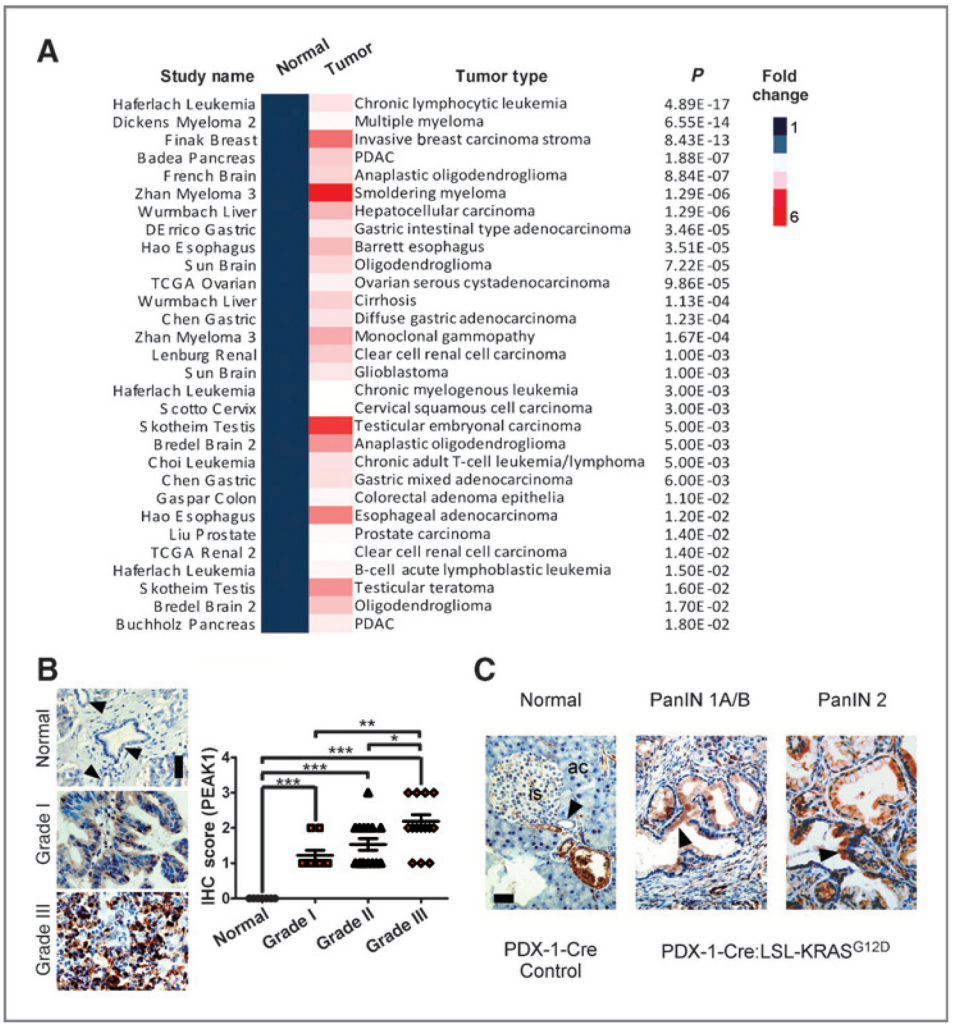

Figure 1.

PEAK1 is overexpressed in multiple human malignancies and is an early biomarker for PDAC development and progression. A, heatmap of fold change in PEAK1 expression in tumor samples. Data are publicly available on Oncomine, and citations are included in Supplementary Data. B, immunohistochemistry of PEAK1 in human PDACs or normal pancreatic tissue sections (left). Arrowheads indicate normal ductal epithelium. Scale bar, 50 μm. Quantitative analysis of immunohistochemical staining for 7 normal, 9 grade I, 15 grade II, and 16 grade III human samples by blind scoring on a scale of 0–3 (right). C, immunohistochemistry of PEAK1 in normal PDX-1-Cre control mice (ac, acinar cells; is, islet) and PanIN 1A/B and 2 from 6 month-old PDX-1-Cre:LSL-KRAS^{G12D} mice. Arrowheads indicate normal ductal epithelium or PanIN lesions. Scale bar, 50 μm.*, **, and *** represent *P* values of < 0.05, 0.01, and 0.001, respectively, as determined by a one-way ANOVA. IHC, immunohistochemical.

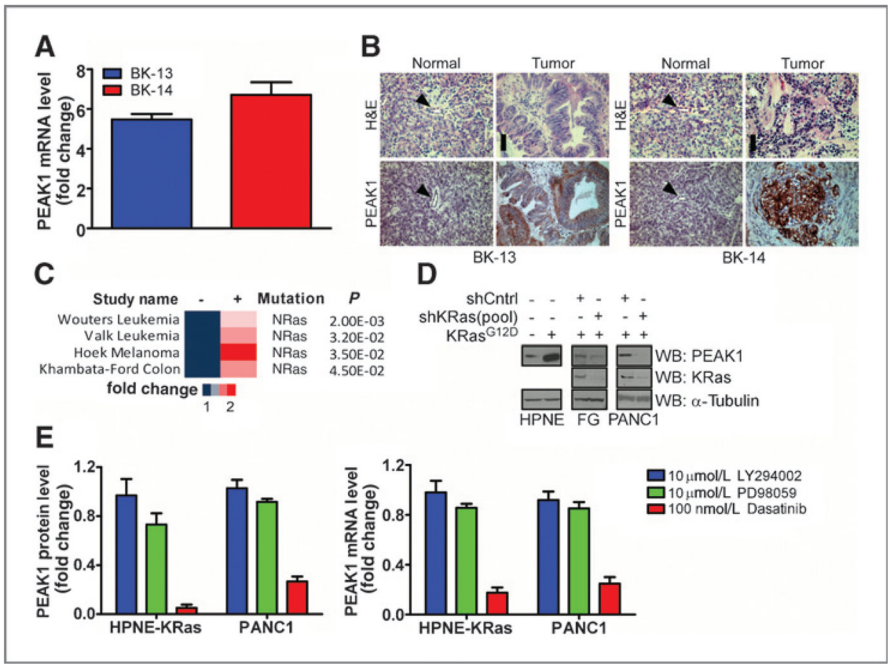

Figure 2.

KRas induces Src-dependent PEAK1 expression in PDAC and other human malignancies. A, qPCR analyses of PEAK1 in oncogenic KRas-containing PDAC tissues collected from patients BK-13 and BK-14 relative to normal pancreas tissue from the same patients. Error bars, SD over 3 analyses. B, hematoxylin and eosin (H&E) staining and PEAK1 immunohistochemistry of tissues from patients BK-13 and BK-14. C, heatmap of fold change in PEAK1 expression in tumor samples with and without oncogenic Ras mutations. Data are publicly available on Oncomine, and citations are included in Supplementary Data. D, Western blot (WB) analysis for PEAK1 and KRas in HPNE (11, 19) or PDAC cell lines (FG and PANC1). E, quantification of protein (left) and mRNA (right) levels of PEAK1 following administration of indicated pathway inhibitors in HPNE-KRas and PANC1 cells, relative to dimethyl sulfoxide (DMSO) vehicle control.

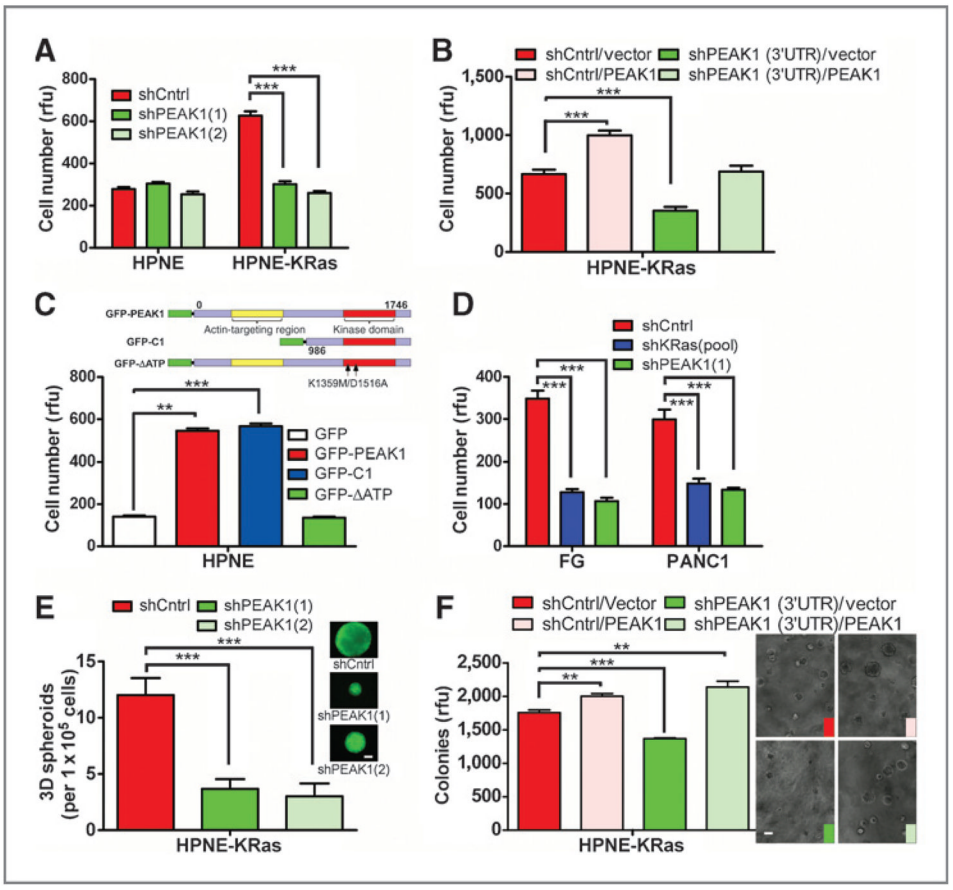

Figure 3.

PEAK1 is necessary for KRas-induced anchorage-dependent and -independent growth of pancreatic cancer cells. Analysis of viable cell number in HPNE or HPNE-KRas cells containing control or PEAK1 shRNAs (A); HPNE-KRas cells containing control or a 3′UTR-targeting PEAK1 shRNA with or without PEAK1 (B); or HPNE cells transiently transfected with, GFP, GFP-PEAK1, GFP-C1, or GFP-ΔATP constructs (C). D, analysis of viable cell number in PDAC cell lines (FG and PANC1) containing control, PEAK1, or KRas shRNAs. E, quantified 3D spheroid suspension growth of HPNE-KRas (insets are representative images for each group) containing control or PEAK1 shRNAs. Scale bar, 200 μm. F, quantified soft agar growth of HPNE-KRas cells containing control or a 3′UTR-targeting PEAK1 shRNA with or without overexpressed PEAK1 (insets are representative images for each group). Scale bar, 100 μm. *, **, and *** represent *P* values of < 0.05, 0.01, and 0.001, respectively, as determined by a one- or two-way ANOVA. rfu, relative fluorescence units.

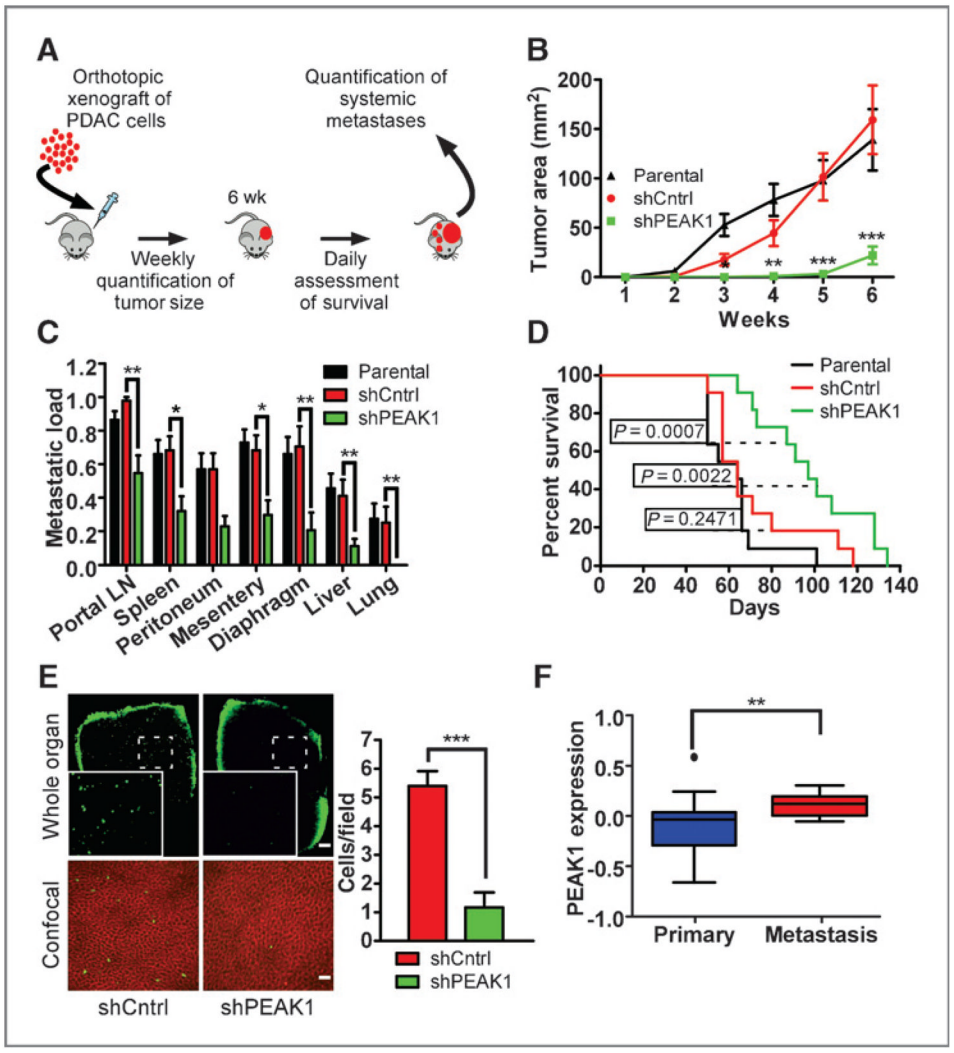

Figure 4.

PEAK1 is necessary for tumor formation, progression, and metastasis *in vivo*. A, schematic of orthotopic implantation model of pancreatic cancer and experimental design. B, parental, shCntrl, or shPEAK1 FG cells were orthotopically implanted into the pancreata of athymic mice ($n = 11$ per group) and imaged over 6 weeks to assess tumor growth. C, normalized metastatic load was calculated as described in Supplementary Materials and Methods and plotted for indicated tissues after harvesting and fluorescence imaging analysis. D, Kaplan–Meier curves were generated to analyze statistical significance of animal survival as described in Materials and Methods. E, PEAK1-mediated metastasis was further assessed by injecting HPNE-KRas shCntrl or shPEAK1 cells into the chicken CAM veins. The liver was removed and imaged 48 hours later with wide-field (top) and confocal (bottom) microscopy to quantify cell metastasis (right). Images are representative of 5 chickens in each group. Scale bar, 2 mm (top) and 200 μm (bottom). F, Tukey plot of normalized PEAK1 gene expression (downloaded from Oncomine) in primary tumor samples in comparison with lymph node (LN) and liver metastases from patients with PDAC; citations are included in the Supplementary Data. *, **, and *** represent *P* values of < 0.05, 0.01, and 0.001, respectively, as determined by one-way ANOVA or Student *t* test (F).

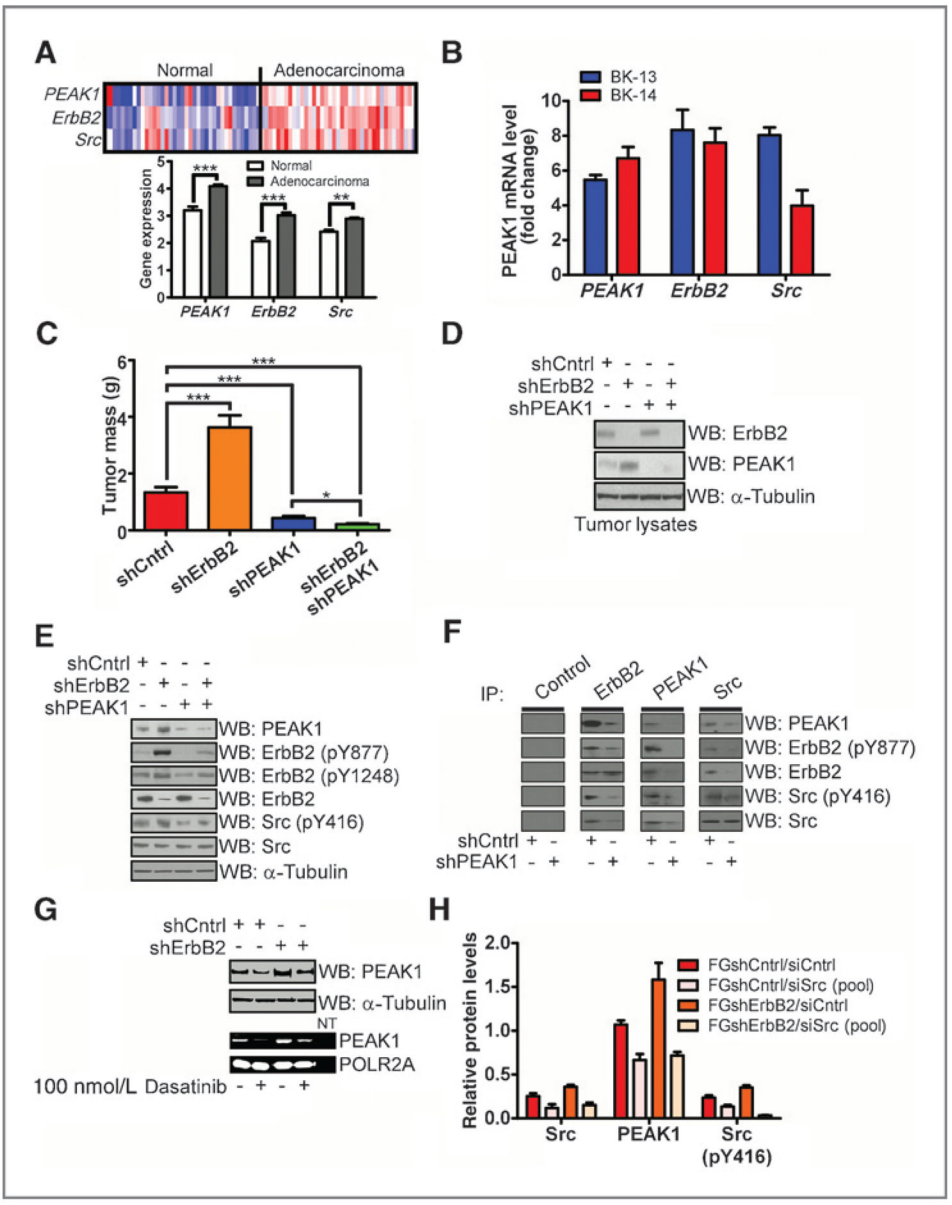

Figure 5.

PEAK1 compensates for ErbB2 loss *in vivo* via Src signaling. A, heatmap and average PEAK1, ErbB2, and Src expression patterns in PDAC and normal pancreatic tissue. Data are publicly available on Oncomine, and citations are included in Supplementary Data. B, qPCR analysis of indicated genes in PDAC tissue from patients BK-13 and BK-14 in relation to normal pancreas tissue from the same patient. Error bars represent SD over 3 analyses. C, average pancreatic tumor mass was measured 6 weeks after orthotopic implantation of FG cells, containing the indicated shRNAs into athymic mice. D, Western blot (WB) analysis of PEAK1 and ErbB2 protein levels from representative tumor lysates. E, Western blot analysis of indicated proteins and phosphoproteins from FG cells containing the indicated shRNAs. F, coimmunoprecipitation (IP) and Western blot analysis of an endogenous, active Src/PEAK1/ ErbB2 signaling complex from FG cells transduced with shCntrl or shPEAK1 constructs. G, Western blot and RT-PCR analyses of PEAK1 levels in FG shCntrl and shErbB2 cells following dasatinib inhibition of Src kinase. H, quantification of indicated

protein or phosphoprotein levels in shCntrl and shErbB2 lysates from FG cells transiently transfected with siCntrl or siSrc (pool) oligonucleotides. *, **, and *** represent *P* values of < 0.05, 0.01, and 0.001, respectively, as determined by a one-way ANOVA or Student *t* test (A).

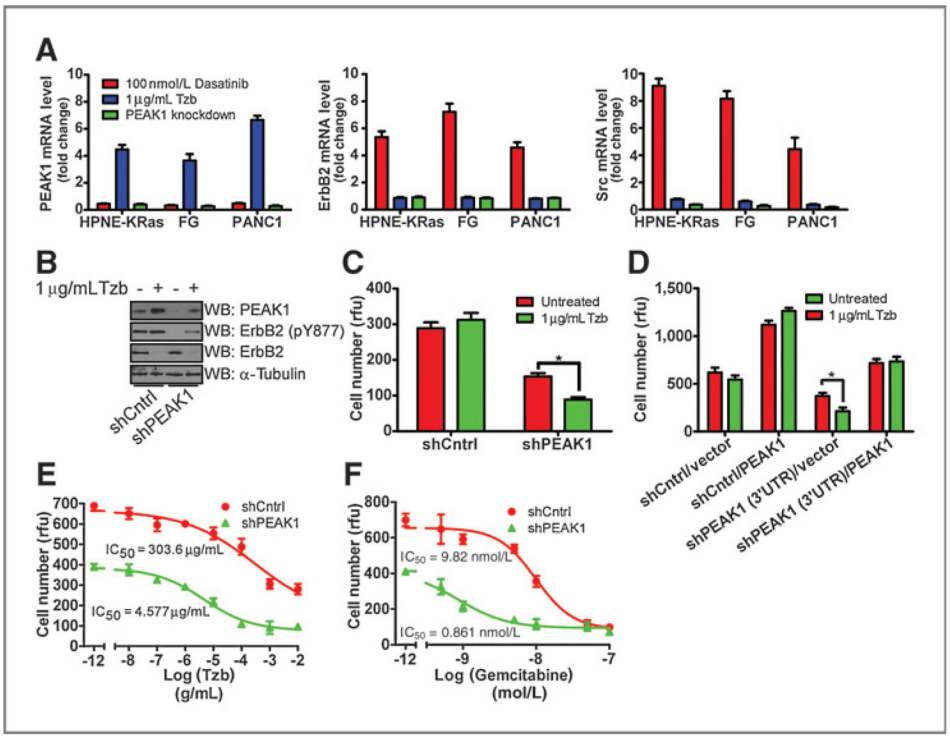

Figure 6.

Src/PEAK1/ErbB2 signaling drives trastuzumab (Tzb) and gemcitabine resistance in pancreatic cancer cells. A, qPCR analysis of PEAK1 (left), ErbB2 (middle), and Src (right) in indicated cells lines following Src, ErbB2, or PEAK1 inhibition relative to the appropriate vehicle-treated or shRNA controls. Western blot analysis (B) for indicated proteins in or viable cell number analysis (C) of PANC1 cells containing shCntrl or shPEAK1 constructs following 72-hour treatment with 1 μg/mL trastuzumab or left untreated. D, analysis of viable cell number in HPNE-KRas cells containing control or a 3′UTR-targeting PEAK1 shRNA, with or without PEAK1 treated with 1 μg/mL trastuzumab or left untreated. Dose–response analyses of trastuzumab (E) and gemcitabine (F) effects on FG shCntrl or shPEAK1 cell number. *, *P* value of < 0.05, respectively, as determined by a two-way ANOVA. rfu, relative fluorescence units.